Optical Communications Telescope Laboratory (OCTL) Support of Space to Ground Link Demonstrations

Abhijit Biswas[1], Joseph M. Kovalik[2], Malcolm W. Wright[3], William T. Roberts[4]

Jet Propulsion Laboratory, California Institute of Technology, Pasadena, California, 91109

The NASA/JPL Optical Communication Telescope Laboratory (OCTL) was built for dedicated research and development toward supporting free-space laser communications from space. Recently, the OCTL telescope was used to support the Lunar Laser Communication Demonstration (LLCD) from the Lunar Atmospheric Dust Environment Explorer (LADEE) spacecraft and is planned for use with the upcoming Optical Payload for Lasercomm Science (OPALS) demonstration from the International Space Station (ISS). The use of OCTL to support these demonstrations is discussed in this report. The discussion will feed forward to ongoing and future space-to-ground laser communications as it advances toward becoming an operational capability.

I. Introduction

Free-space laser communications has made impressive strides in the past two decades and continues to emerge as a game changing technology for servicing science, exploration and commercial ventures from space. In accordance with these developments, space-to-ground demonstrations are being pursued by several space agencies. Two recent demonstrations sponsored by the National Aeronautics and Space Administration (NASA) are the Lunar Laser Communication Demonstration (LLCD) and the Optical PAyload for Lasercomm Science (OPALS). The primary phase of the LLCD demonstration was completed during October-November 2014 while the OPALS flight system (FS) is awaiting launch from Kennedy Space Center (KSC) at the time of writing this paper.

The NASA/JPL Optical Communications Telescope Laboratory (OCTL) located at Table Mountain, CA served as an alternate ground terminal for LLCD with the primary terminal being at Whitesands, NM. OCTL is now ready to support the upcoming OPALS demonstration. OCTL has been used for space-to-ground link demonstrations from the Laser Utilizing Communications Experiment (LUCE) terminal on the Japanese Aerospace Exploration Agency (JAXA) Optical Inter-orbit Communications Engineering Test Satellite (OICETS) spacecraft in May 2009[1, 2]. The use of OCTL as a ground station is also planned for NASA's future Laser Communication Relay Demonstration[3] (LCRD). Farther in the future NASA plans to fly a deep-space optical communication technology demonstration, though a specific mission is yet to be identified. For this class of missions the use of OCTL as a laser transmission terminal is planned. In this paper the operational characteristics of OCTL for supporting LLCD and OPALS will be presented.

For LLCD[4] the Lunar Lasercom Space Terminal (LLST) on-board LADEE was capable of maximum downlink data-rates of 622 Mb/s to the primary Lunar Lasercom Ground Terminal[5] (LLGT). Two alternate terminals were fielded in order to provide weather and cloud diversity to increase contact time from space. One of them using OCTL was called the Lunar Lasercom OCTL Terminal[6] (LLOT) and supported downlink rates of 39 and 78 Mb/s. The second alternate terminal[7] used the European Space Agency owned Optical Ground Station (OGS) at Tenerife, Spain.

---

[1] Sr. Optical Engineer, Optical Communication Group, MS 161-135, 4800 Oak Grove Drive, Jet Propulsion Laboratory, Pasadena, CA.

[2] Sr. Optical Engineer, Optical Communication Group, MS 161-135, 4800 Oak Grove Drive, Jet Propulsion Laboratory, Pasadena, CA.

[3] Sr. Optical Engineer, Optical Communication Group, MS 161-135, 4800 Oak Grove Drive, Jet Propulsion Laboratory, Pasadena, CA.

[4] Sr. Optical Engineer, Optical Communication Group, MS 161-135, 4800 Oak Grove Drive, Jet Propulsion Laboratory, Pasadena, CA..

The OPALS demonstration[8] was developed under the Jet Propulsion Laboratory (JPL) Phaeton Program under which entry level engineers are trained in JPL processes for developing and implementing space missions. The OPALS Project objective was to demonstrate a laser communication link from the International Space Station. OCTL was chosen as the ground station for this demonstration and the nominal downlink data-rate is 50 Mb/s.

The organization of the remainder of this paper is as follows. In Section II the OCTL telescope characteristics and control are described. Section III provides a discussion of the system considerations that factor in the OCTL configuration. In Sections IV considerations relevant to optical trains for coupling the laser

II. OCTL Telescope Characteristics and Control

A. Telescope Facility

OCTL is located at JPL's Table Mountain Facility in the San Gabriel Mountains near Wrightwood, California. The site can fully support optical telescope operations with 24/7 availability and accommodations for sleeping. The location is convenient to JPL since it is only about a 1.5 hour drive away. OCTL has line of sight to numerous ground locations which permit point to point field testing with ranges of a few hundred meters to a few kilometers. The telescope laboratory is equipped with a full suite of optical, electronic and mechanical tools and test equipment.

The networking capability at OCTL was recently upgraded from standard internet access to a secure JPL mission connection. This upgrade included dedicated router hardware and controlled building access through a badge reader. A local computer with a firewall to the JPL Mission Operations Center acts as a data server to both transmit and receive data at rates up to a few hundred kilobits/second that are limited by the T1 internet service. Secure voice connection is also possible using VOIP over this connection.

The OCTL telescope itself has a 1m diameter primary mirror mounted on a fast-tracking elevation over azimuth gimbal with a coudé path that sends the collected light signal into a controlled laboratory area. The focal ratio of the telescope is F/76 (F/ represents the focal ratio) with a near diffraction limited field-of-view (FOV) of over 500 μrad (38 mm at the telescope focus) and a seeing limited unvignetted FOV of approximately 2.6 mrad (200mm at focus). By translating the secondary mirror, the telescope is capable of being focused at conjugate distances ranging from infinity down to less than 1 km. Table Mountain Observatory is located (34.4°N latitude, 242.3E longitude) at nearly 2300 meters. The telescope has a clear view of the sky at all azimuth angles above 0 to10 degrees elevation, with the local tree line restricting 0-degree viewing at some azimuthal angles. Weather and astronomical seeing information is available from instruments located at the site. The gimbal can slew at up to 20 degrees/sec in azimuth and 10 degrees/sec in elevation. The all sky blind pointing error is less than 17 μrad (1σ). The telescope also has a co-aligned 20 cm diameter, F/7.5 Classical Newtonian acquisition telescope which can accommodate auxiliary instrumentation. This telescope provides an unvignetted FOV at the focal plane of 5 mrad. Co-alignment of this telescope with the main OCTL telescope is usually better than 100 urad, which easily supports acquiring and guiding sources into the main telescope field of view.

Both electrical and fiber optic cables and fiber optic cables that wrap through the telescope mount service loop connect the telescope to the operator control room. Telescope operations can take place both during day and night and the telescope can point to within 5 degrees of the sun without any solar damage.

The final mirror in the telescope coudé path (M7, see Figure 1b below) can rotate to four different positions which each lead to separate optical benches. This allows concurrent development, integration and testing of four different optical receive/transmit assemblies (more if space allows the sharing of an optical bench). Furthermore multiple mission operations can be supported in the same time period as long as they do not occur simultaneously. An AR-coated fused silica window in the optical path prevents the exchange of air between the telescope dome and the coudè room, and prevents the potential chimney effect from degrading the telescope seeing.

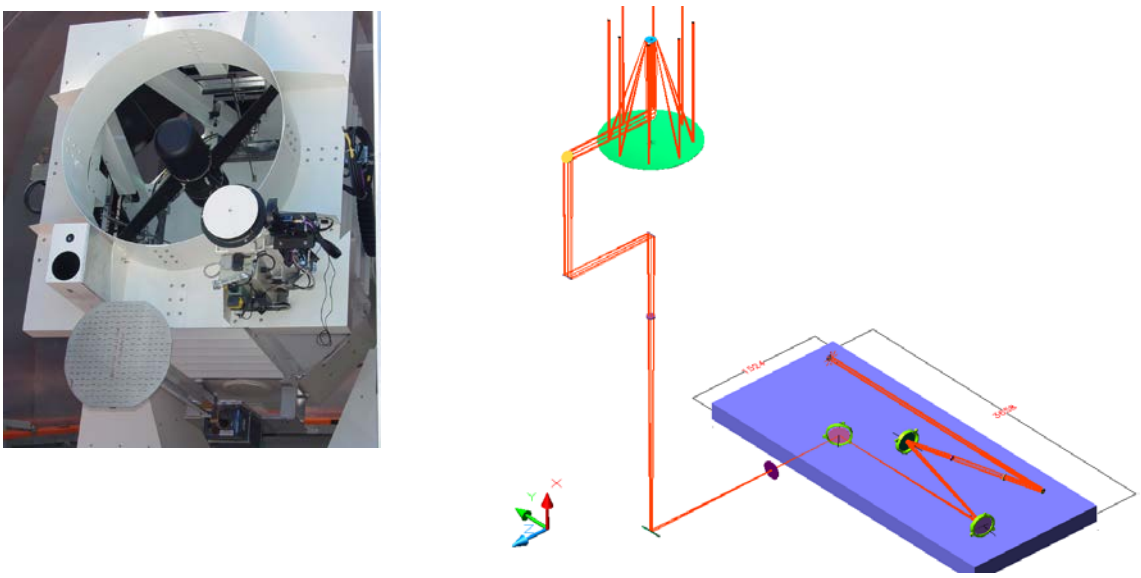

(a) (b)

Figure 1 (a) Front view of the OCTL telescope showing the secondary obscuration (S) the acquisition telescope (AS), the weather radar antenna (R) and the Infra-red cameras (IRC); (b) a schematic view of the coudè configuration showing the seven telescope mirrors M1 through M7 with a view of light being coupled to one of the four optical benches.

B. Telescope Control System

OCTL uses a computer controller with a real time operating system. Besides the main telescope function of accurate pointing, the telescope provides many ancillary controls for telescope operation including:

- safety control features such as pneumatically actuated brakes to stop the telescope from moving and a shutter to cover the primary mirror of the telescope
- sun avoidance system to prevent the telescope from pointing to within a programmable angular distance
- mount calibration procedure
- control of the M7 position
- control of auxiliary systems such as the acquisition telescope focus and power to accessories mounted on the telescope
- slaving of the dome to telescope motion

Originally, the telescope controller interfaced to a motion control system that operated both the dome and primary focus. However, this functionality now uses a separate dedicated motion controller in order to enhance operational reliability.

A graphical user interface allows an operator to use the telescope. In addition to controlling the various telescope systems, it also has three tracking modes:

- sidereal tracking where it can follow a star right ascension and declination
- Two Line Element (TLE) tracking where the telescope can track a NORAD TLE ephemeris
- state vector tracking where the telescope follows an ephemeris defined in a file with time, azimuth and elevation entries

Unfortunately, this interface does not allow dynamic, real time updates to the telescope tracking. A recent upgrade to the telescope controller added a Reflective Memory Interface (RMI) to the real time computer. A twin RMI card connected via a fiber optic cable and located in a remote computer can both read and write to the telescope controller computer. This remote computer can emulate all the functionality of the telescope controller. Moreover, it can command the telescope azimuth and elevation in real time as if the telescope were a "smart" gimbal.

Figure 2 shows a block diagram of the telescope control system. The telescope currently has two CCD cameras that are connected to the control room via firewire-to-fiber optic interface. One camera images the acquisition telescope while the other is attached to a retrofitted motorized zoom lens (not shown in Figure 1) that can be adjusted remotely in the control room. The zoom lens camera has a 34 degree to 1.7 degree field of view. The camera exposure time and gain can be set by the user in the control room. The wide range in field of view is useful when trying to locate objects, especially during field testing. It also simplifies acquisition and tracking of moving

objects like airplanes by starting with the zoom camera and a wide field of view; zooming to a narrow field of view; and then handing the tracking to the acquisition telescope camera.

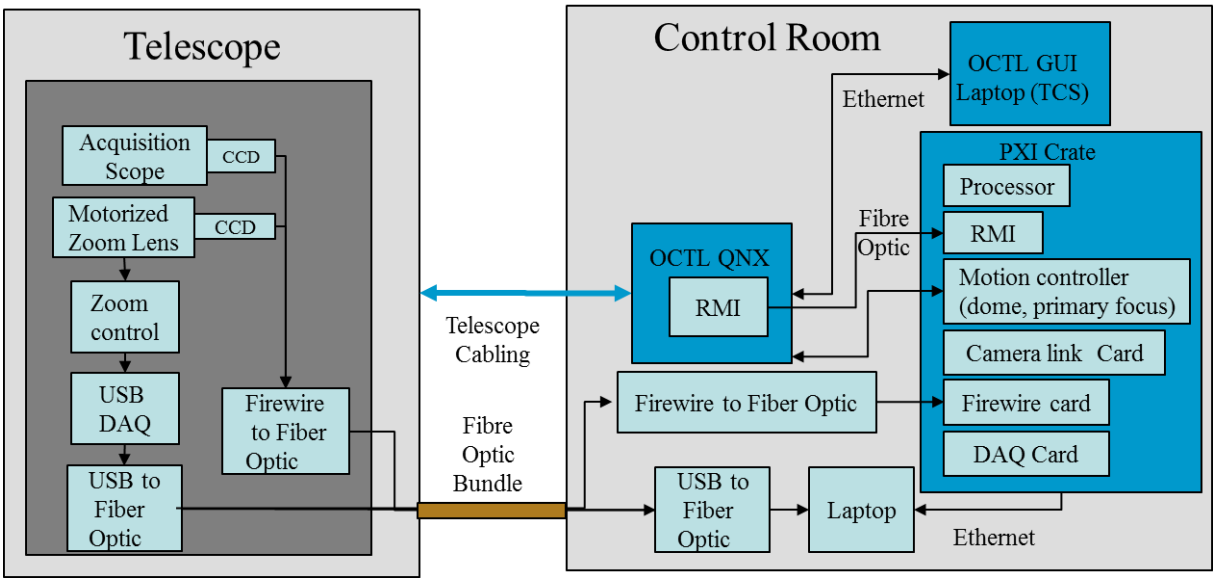

Figure 2 Block diagram of telescope control system

The control room computer systems are designed to allow different experiments to interface to the telescope. The OCTL QNX real time controller is the main processor for the telescope system. It is connected to the OCTL GUI laptop which retains most of the functionality of the original telescope interface. The RMI card from the OCTL QNX controller has its mirror in a PXI based real time computer controller. A laptop computer acts as a host to the target PXI system. All commanding and data products flow through this laptop. While the laptop currently sits next to the QNX computer controller, it could be used to operate remotely through an internet connection.

Besides the computer processor and RMI card, the PXI crate hosts numerous standard interface boards including:

- A motion controller card that drives the telescope primary focus and the telescope dome. Inputs from the OCTL QNX controller allow an auto adjustment of the telescope focus and a dome motion slaved to the telescope azimuth position.
- A cameralink card to control and receive images from an imager
- A firewire card to control and receive images from an imager
- A data acquisition card with analog and digital inputs and outputs

While the laptop computer can receive any pointing information format and convert it into a telescope azimuth and elevation, the current system can perform state vector tracking with the same format as the original telescope system and sidereal tracking. The telescope can feedback the centroid positions of objects from any of the imagers (zoom, acquisition or main telescope) to center the objects and track them.

Figure 3 shows a functional block diagram used for the LLOT at OCTL. In this case, the laptop or LLOT controller acts as an overall host for the different sub-systems and data manager for telemetry. Via a TCP/IP protocol it commands a separate computer in the coudé room which locally controls and monitors uplink lasers, the beam divergence zoom system and the variable beamsplitter that splits the light between the tracking camera and the InGaAs camera imager (these are described in more detail in Figure 9 in Section IV).

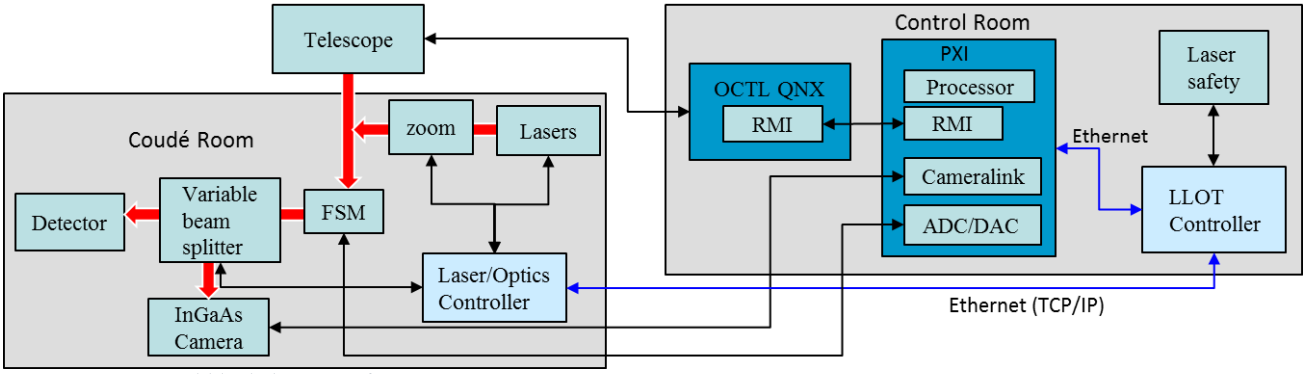

Figure 3 Functional block diagram of LLOT experiment at OCTL

The PXI processor in Figure 3 reads the InGaAs camera and performs a centroid calculation of the downlink spot. The PXI processor then uses this centroid to center the spot by commanding the Fine Steering mechanism (FSM). The FSM command signal is also sent to the telescope controller where it adjusts the telescope pointing in order to offload any offset that accumulates on the FSM. Since there is no point ahead mirror in this setup, the telescope itself must point ahead to the spacecraft. The FSM then looks behind with a programmed offset from the LLOT controller. The mission operations center provides a time-stamped file with both the point ahead and look behind coordinates that are read by the LLOT controller.

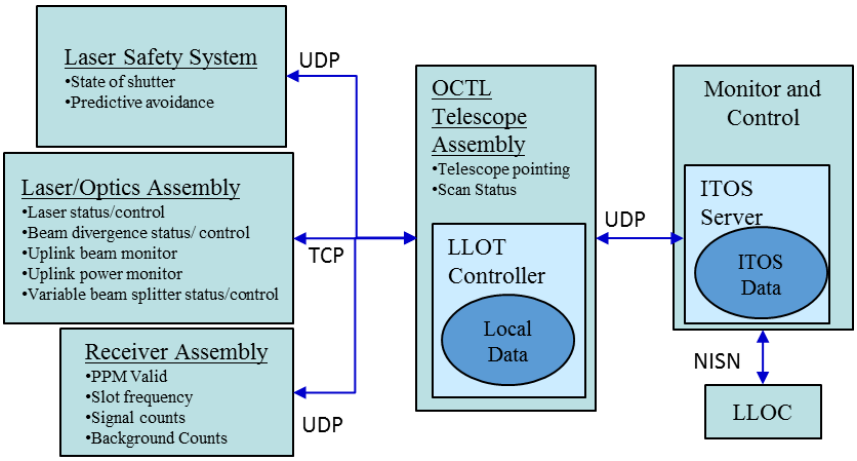

Figure 4 Telemetry flow for LLOT experiment at OCTL

Figure 4 shows the telemetry flow for the LLOT experiment at OCTL. The LLOT controller receives data from the laser safety system, the laser /optics assembly computer and the receiver assembly. It also incorporates data from the PXI system controller. It then assembles this data into CCSDS packets and frames which are sent to a monitor and control server that runs ITOS (Integrated test and Operations Software) telemetry processing software. This server then forwards the CCSDS data to the operations center (LLOC) over a secure network connection. The server also receives telemetry form the LLOC and displays it. Both the transmitted and received data are stored locally in the monitor and control server.

C. Telescope Pointing and Tracking

A semi-automated mount calibration procedure allows an operator to choose stars distributed across the sky; center them in the primary imager; and then record the telescope position. A commercial software package then uses this data to produce a mount calibration algorithm. Figure 5 shows the blind pointing performance for stars and a satellite. The telescope pointed to fifty stars and the offset position centroid was recorded. The mean radial error was 9.5 µrads ±29 µrads (1σ). Laser ranging stations track geodetic satellites and create accurate ephemeris data sets. In this case, the telescope pointed to a sunlit pass of Ajisai. The satellite reflects glints of sunlight from its solar panels which produces a blinking image on the telescope. The mean radial tracking error across a pass was 1.1 µrads ±10.7 µrads (1σ).

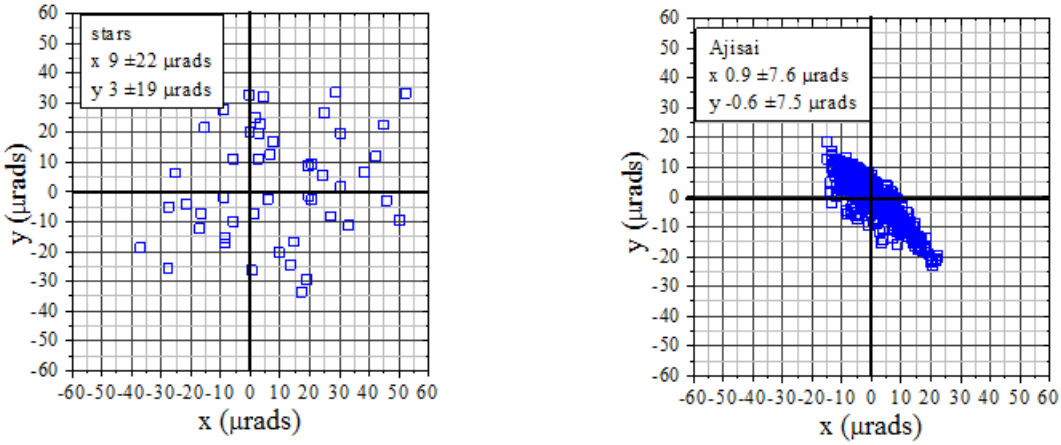

Figure 5 Blind pointing performance for 50 stars distributed across the sky and a geodetic satellite, Ajisai

Another tracking test involved blind pointing to the International Space Station (ISS), in preparation for the upcoming OPALS demonstration, during a sunlit pass. In this case, a pointing file was generated at JPL by propagating the ISS location from a time less than an hour before the start of the pass. Since the ISS is in a low orbit and has a very big cross section, it suffers from a fair amount of drag and ephemeris predictions become stale after a few orbits. Figure 6 shows an image of the ISS taken near zenith.

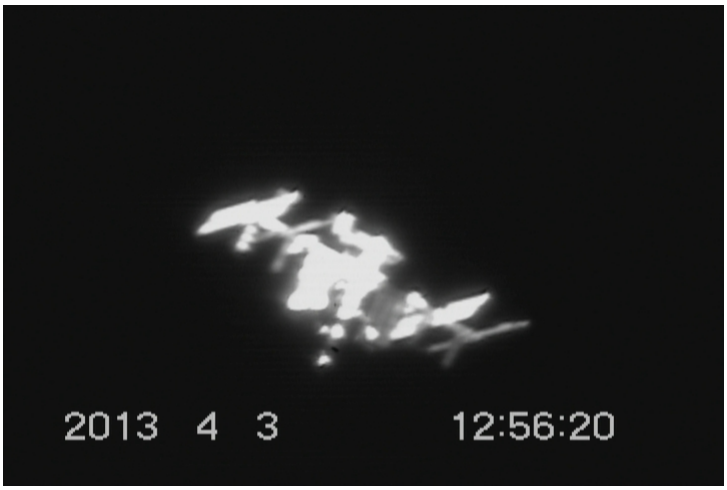

Figure 6 ISS image taken near zenith with telescope blind pointing to a JPL generated ephemeris file

The closed tracking performance of the telescope was tested using the centroid from a star image. Figure 6 shows the full nested feedback control using both the FSM and telescope offload. The effective camera tracking has a radial tracking error of ±0.8 µrads (1σ) which corresponds to effective motion of the received spot on the detector. The telescope itself has a pointing error ±2.7 µrads (1σ) in azimuth and ±4.1 µrads (1σ) which corresponds to the effective pointing error of the outgoing laser beam.

Ephemeris pointing uncertainties and/or blind pointing errors can result in uplink lasers completely missing their intended target depending on the beam divergence being transmitted. Since the spacecraft can have its own pointing uncertainties, a step stare scan approach allows the spacecraft to continuously scan its uncertainty region while the ground telescope scans through its uncertainty with a dwell at each offset position that is greater than the spacecraft scan time. Figure 8 shows two different scan types with a star acting as reference target. In each case, the step size, dwell time and scan length can be set through the LLOT controller.

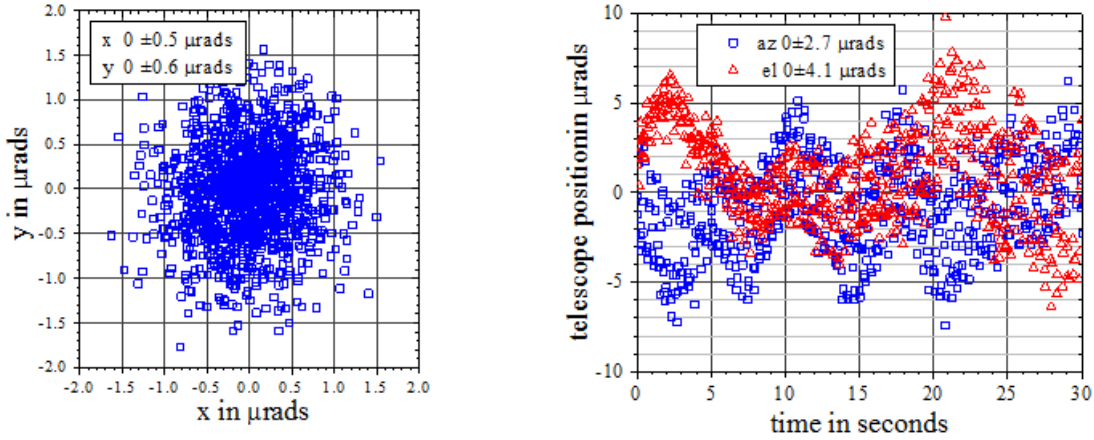

Figure 7 the left hand graph shows a xy plot of closed loop tracking of a star using the FSM and telescope offset. The right hand graph shows deviation of the telescope azimuth and elevation readback from sidereal tracking

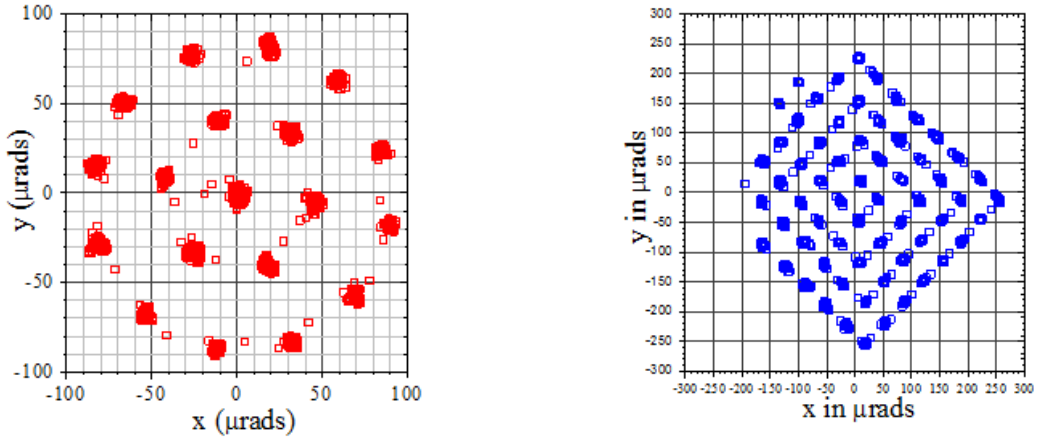

Figure 8 the left hand graph shows a hexagonal step stare scan while the right hand graph shows square spiral step stare scan.

III. System Considerations for Transmitting and Receiving Lasers

A. Overview

The telescope optics and control capabilities briefly described in Section II afford different laser communication ground terminal architectures. The 1m diameter aperture provides adequate collection area for expected laser signals from near-Earth, lunar and Lagrange point satellites[9], even though there has not been any experience with the latter. For deep-space ranges beyond 0.1 AU the collection area is inadequate for data-rates supported by typical flight transceivers. However, OCTL with its mount characteristics can support transmitting kilowatt class laser power for delivering beacon and uplink signal to deep-space[10].

For near-Earth links, specifically LLOT and the OPALS Ground Station (GS), a mono-static architecture was implemented where a common aperture is used for transmitting the beacon and receiving the downlink. The mono-static architecture lends itself to easier receive/transmit co-alignment. Adequate optical isolation must be implemented with a mono-static configuration so that the transmitted beacon backscattered from optics, telescope, surfaces and atmospheric aerosols does not contribute unacceptable additive noise on the receiver or acquisition/tracking sensors used with the receiver optics.

As mentioned earlier the coudè configuration of OCTL offers the advantage of providing optical and instrument designers a laboratory bench development and operations environment in addition to allowing the development of multiple setups that do not operate concurrently. In order to provide this convenience the optical transmission through the telescope must account for losses from 7 surfaces. Since many of these surfaces are exposed to the elements, a practical limitation becomes rather substantial optical transmission losses as will be elaborated in Section IV below.

Each link design involves unique system requirements and we will briefly discuss for LLOT and OPALS GS next.

B. LLOT System Requirements

The link design for LLOT has been reported[6] recently. The downlink power received at 1550 nm from a distance of approximately 400,000 km was 25-160 pW. Average beacon laser power on the bench-top was approximately 25-30 W at 1568 nm. Since receive and transmit optical paths shared common optical elements and in order to prevent beacon backscattered or back-reflected light from overwhelming the downlink signal an optical isolation of at least 126 dB was required. This was one of the key design requirements for the optical train design.

The required mean beacon irradiance at the LLST aperture, on-board LADEE, for acquisition and tracking were 3.6 and 36 nW/m^2 for tracking. The beacon is modulated at 1 kHz in order to allow the LLST detector to reject background. The LLST also received uplink data at 20 Mb/s; however, LLOT was not equipped with the capability to transmit uplink. The uncertainty in spacecraft ephemeris and telescope mount pointing accuracy together with available power based on availability of lasers required a variable beam divergence of 40-110 μrad. The wider beam ensured acquisition with the option of scanning. The narrower beam divergence ensured delivery of sufficient irradiance to support LLST beacon tracking. Furthermore, irradiance fluctuations with deep-fades caused by propagation through the turbulent atmosphere had to be minimized. The LLOT beacon used multiple beams that were transmitted through sub-apertures in the telescope so that each incoherent beam traversed a diverse atmospheric path, averaging out the fluctuations when the beams recombined in the far-field. Multi-beaming combined with margin over the mean required irradiance was implemented in order to mitigate beacon fading due to atmospheric turbulence.

Once the beacon was acquired by LLST the downlink laser beam was pointed back to LLOT. 0.5 W average laser power was transmitted from LLST resulting in 25-160 pW of received power at LLOT after variable atmospheric attenuation and fixed telescope and optical losses. The signal was initially spatially acquired on an array sensor where centroid computations described in Section II helped adjust "point-behind" angles so that the signal could be directed to a detector/receiver assembly. Downlink incidence on the LLOT detector initiated communication reception of the 16-ary pulse-position modulated (PPM) LLST[4] signal. As mentioned earlier the data-rates received by LLOT were 39 and 78 Mb/s. A serially concatenated pulse-position modulation (SCPPM) near capacity achieving forward-error correction code was used. The uplink data transmission at 10-20 Mb/s from LLGT was used by to lock the clock on LLST. Since LLOT was a late-comer to LLCD, modifications to LLST to support no uplink could not be made. So the downlink received at LLOT had a drifting clock since the voltage controlled oscillator temperature did not stabilize over the duration of the pass. A requirement for the LLOT receiver was to accommodate this clock drift at rates determined during ground testing.

Typical OPALS link durations were about 20 minutes with angular slew rates of a few-hundredth of a degree per second. LLOT operations were coordinated by LLOC as indicated in Figure 4. For example, signal power detected by the LLST quadrant detector is telemetered to the LLOC over a RF link and relayed back to OCTL. Thus in near real-time the beacon signal delivered from LLOT could be verified and needed adjustments could be made if necessary.

C. OPALS System Requirements

The OPALS[8] GS will also use a mono-static configuration, receiving 1550 nm from the ISS and transmitting a 976 nm beacon. The wider spectral separation of downlink and uplink made optical isolation on the ground easier. The 976 nm beacon was chosen so that a low cost silicon camera can be used by the OPALS FS. From an atmospheric propagation viewpoint higher wavelengths usually have higher atmospheric transmission and are less vulnerable to atmospheric turbulence. The lower range to the ISS was traded for the lower performance of a 976 nm beacon. The OPALS range is nominally 800 km and both downlink and beacon lasers use wider beam-divergence. Consequently the OPALS flight system (FS) will use a low complexity implementation relying on coarse pointing of a 1 mrad downlink laser with a gimbal. The OPALS beacon is also a multi-beam beacon in order to mitigate turbulence, however, the beam divergence transmitted to the ISS is 1.6 mrad. Transmitting wider beam divergence is more forgiving on pointing and is also less vulnerable to atmospheric turbulence. The OPALS beacon is a continuous wave laser and a combination of higher power transmitted from the ground and spectral filtering on the flight terminal on-board ISS will be used to reject background. The OPALS links also do not involve pointing close to the sun as was the case for LLST.

The OPALS link will be unidirectional from space-to-ground and will operate at a nominal data-rate of 50 Mb/s using on-off-key modulation with a Reed-Solomon forward error correction code. The link design for OPALS

results in 10's of nanowatts of downlink power that can be received using commercial detectors and receivers. The decoding will be done using software.

The accommodation of the OPALS FS on the nadir pointed ISS location imposes line-of-sight restrictions due to obstructions and laser safety to avoid irradiating ISS surfaces with 1 W of laser power output by the FS. As a result of this typical OPALS link durations are about 100 seconds. Of course the slew rates for OPALS GS are much higher than LLOT and can approach 2 deg/sec on near overhead passes.

IV. Optical Train for Transmitting and Receiving Lasers

A. LLOT Optical Layout

The main OCTL telescope mirrors are FSS-99 protected silver mirrors. Total telescope reflection losses (primary through M7 reflection losses) have been measured to be 2.6 dB at 1550 nm, and 3.1 dB at 976 nm. The more than nominally expected transmission loss is attributed to the age of the coatings (13 years), and the environment to which the primary, secondary and tertiary mirrors are frequently exposed. We have measured the ability of these coatings (on clean witness samples) to withstand up to 100,000 W/cm^2 of tightly-focused, continuous near-infrared laser power without damage. These levels are sometimes necessary in transmitting high-power beacon and communications beams to satellites and probes in deep space.

The LLOT optical layout for coupling light in and out of the telescope is shown in Figure 9. One of the key requirements pointed out for the LLOT design was high optical isolation. This requirement was met with a design that uses high-performance dielectric dichroic filters designed to efficiently transmit the downlink 1550 nm signal to the receive optics while simultaneously reflecting the counter-propagating 1568 nm beacon. The filter was designed for use at a 10-degree angle of incidence, at which we measured a 1550 nm insertion loss of 0.08 dB, and a 1568 nm transmission rejection of at least 72 dB. To ensure sufficient transmit/receive isolation, three of these filters (RNF1, RNF2 and RNF3 in Figure 9) were employed in the receive optical path, one of which sealed off the aperture to a light-tight enclosure that housed the acquisition sensor and multi-mode optical fiber used to couple light to the communication detector. The dichroic filter to seal the aperture of this enclosure rejected stray beacon light scattered around the coudè room. The cumulative insertion loss of these three filters at 1550 nm was measured to be 0.23 dB. The optical isolation measured with this arrangement was at least 130 dB.

The LLOT beacon optics employed 6 combined collimated beams into a parallel-propagating hexagonal arrangement that is incident into the plane of the paper on Fold Mirror 1 in Figure 9 so that the beams are reflected parallel to the bench surface. A zoom system was employed that allowed the beam divergence to vary from 40 μrad to 110 μrad, the former to allow sufficient irradiance at the spacecraft to support spacecraft fine pointing, and the latter to support initial acquisition at a lower irradiance level. Again, the beam propagation system was designed to bring all beams to overlap irrespective of the zoom condition, and at a shallow angle to allow the beams to fit through the F/76 telescope cone with the help of the combining lens and a number of fold mirrors as shown in Figure 9. The beams can be shuttered with the laser safety shutter so that beacon transmission can be interrupted without powering down the lasers. The entire beacon path is also in a light-tight enclosure that contains stray light scattered from mirror surfaces. The amplified spontaneous emission (ASE) filter at the exit of the beacon enclosure blocks spectrally broad ASE that would be transmitted through RNF.

The receive optical train shown in Figure 9 is designed to re-image the telescope focal plane through a variable beam splitter onto an indium gallium arsenide (InGaAs) acquisition camera and/or a 62.5 micrometer core multi-mode optical fiber with a numerical aperture of 0.275. A fast steering mirror is used to correct for point-behind angles as described in Section II. The variable beam splitter uses frustrated total internal reflection by adjusting the air gap between two prisms with a piezoelectric actuator. During initial spatial acquisition all the signal is directed to the camera. Once acquired closed loop tracking is initiated and more than 70% of the downlink signal is directed to the fiber by applying a voltage to the piezoelectric actuator while still maintaining sufficient signal on the camera for tracking. The optical fiber output was optionally coupled to a femtowatt PIN diode or the photon-counting detector assembly described in Section V. Furthermore a counter-propagating 1550 nm laser could also be injected to the multi-mode fiber, during testing, to verify alignment.

Receive/transmit co-alignment for the LLOT was established by centering a star on the acquisition camera and ensuring that it also passed through a stopped down iris at the coudè focus shown in Figure 9. Each of the beacon beams was also focused through the same stopped iris and the spot pattern on dome was inspected to ensure unvignetted transmission through the telescope. With this approach a co-alignment of approximately 2-5 μrad could be maintained. For LLOT commercial off the shelf optical mounts were used and alignment was performed manually. Diurnal temperature fluctuations and mechanical drift required frequent checking of alignment. A

beacon monitoring camera was also used with the aid of which the beacon spots could be re-imaged at a field point conjugate to the telescope focus by splitting off a small fraction of the outgoing beacon with the pellicle beamsplitter. Future systems should automate both the monitor and control of alignment in order to ease operations.

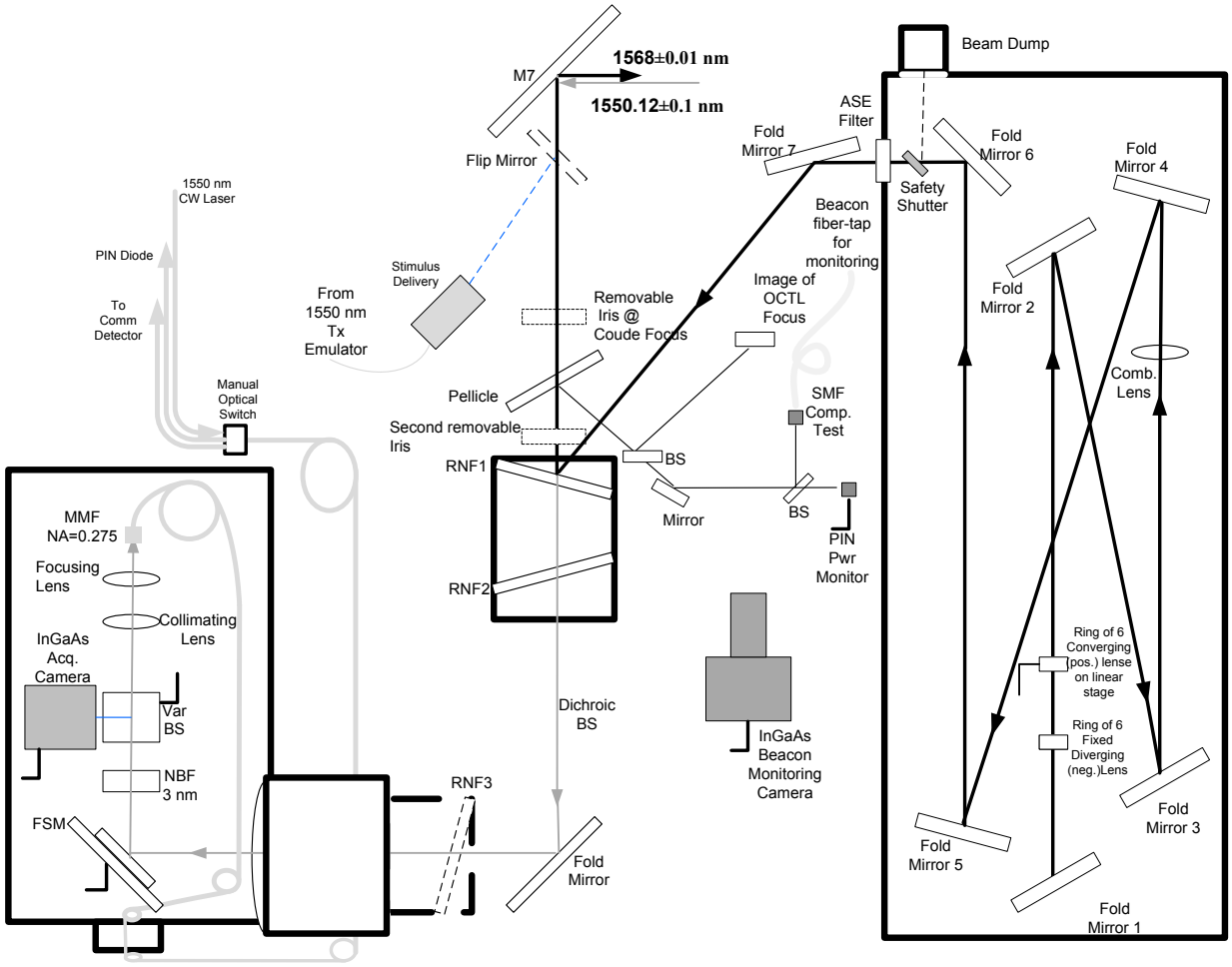

Figure 9 Schematic optical layout for coupling light in and out of the telescope for LLOT operations.

B. OPALS Optical Layout

The optics retrofitted to OCTL for the upcoming OPALS demonstration is shown in Figure 10. Like the OICETS demonstration[1, 2], this link is made to a low-earth-orbiting (LEO) spacecraft. The design employs a 20 cm off-axis paraboloidal (OAP) mirror, similar to the approach followed in the OICETS demonstration. The OAP serves both as a mirror for directing the 1.6 mrad beacon through the narrow telescope, as well as transmitting the downlink field-of-view onto the acquisition camera and the data detector. In this case 4 lasers are co-propagated and the wide beam divergence eases alignment.

The downlink is reflected from the OAP and transmit receive separation is achieved with a dichroic splitter. The downlink is transmitted through the splitter and is incident on a fast steering mirror after which it is split between an InGaAs camera and a commercially available InGaAs avalanche photodiode detector.

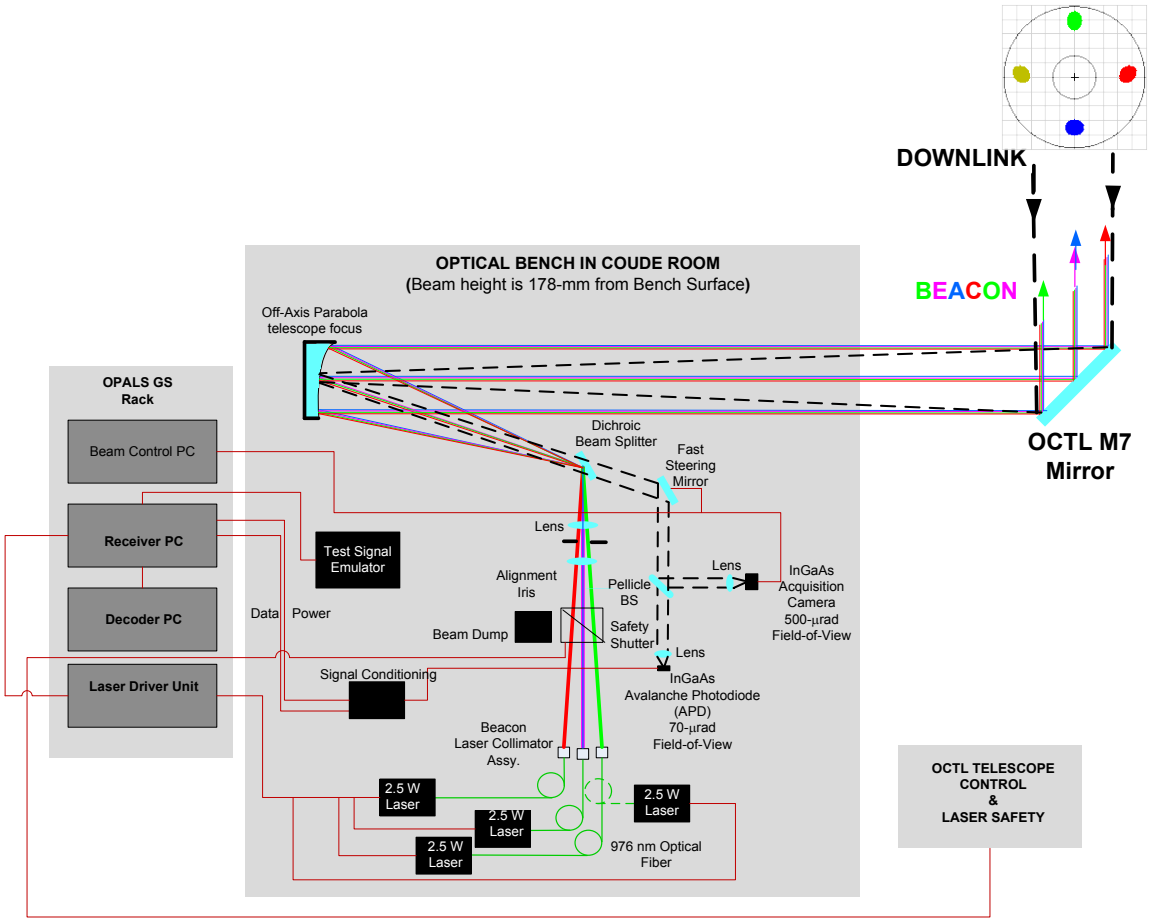

Figure 10 Schematic optical layout for OPALS operations.

V. Optical Receivers & Lasers

A. LLOT Receiver

The LLOT detector/receiver assembly utilized a novel tungsten silicide[12, 13] (WSi) superconducting nanowire single-photon counting detectors (SNSPD) array. A 66 micrometer diameter 12 pixel array to match the 62.5 micrometer multi-mode fiber diameter was used. The nanowire array is held at approximately 800 mK in a closed cycle Gifford-McMahon cryostat. The detectors were maintained at 4 K and prior to a link an evaporation-condensation cycle was used to lower the temperature to 800 mK. The detectors could be maintained at 800 mK for approximately 11 hours. The detector output is amplified by silicon-germanium amplifiers held at 40K and the analog output was fed through the cryostat and a discriminator circuit was used to set a threshold for photon-counting. An analog combining circuit followed the discriminator amplifiers.

The combined analog signal is fed to a high speed digitizer with a 1.25 GS/s sampling rate. The digitized signal is stored using a redundant array of independent disks (RAID). The LLOT receiver was a post-processing software receiver that extracted decoded code-words downlinked from LLST after the pass. A code-word error rate of 1E-5 was targeted. As reported in ref. 6 zero errors were detected most of the time. During the pass, limited concurrent processing was performed by reading blocks of stored data to estimate the slot-clock frequency so that the reception of pulse-position modulation signal at the expected downlink data-rate could be verified in near real-time.

B. OPALS Receiver

The OPALS receiver will use commercially available clock and data recovery (C&DR) circuits to extract the clock from the downlink. The output by the C&DR is digitally stored on a commercial card capable of storing 160 seconds of data at 50 Mb/s. The stored data files can be processed with decoding software that extracts the data. The OPALS objective is to downlink a video file that is stored in the OPALS FS storage memory. The decoder

extracts the video file and can play it back to ensure that the link is working properly. With the Reed-Solomon forward-error-correction an uncoded bit-error rate of < 1E-4 is needed to receive an error free downlink.

As was done for LLOT real-time monitor and control of the link will be implemented for OPALS. In addition to monitoring the outgoing beacon power, the received power will be sampled at kHz rates and stored so that atmospheric turbulence can be evaluated with post-processing analysis. The status of the C&DR circuit will also be monitored to record any loss-of lock due to link interruptions caused due to deep-fades of other system anomalies.

C. OCTL Laser Transmitters

Ground laser transmitters are tailored for each experiment and vary from semiconductor diode lasers to high power solid state laser systems in either a continuous wave (cw) or pulsed mode depending on the link requirements. Ranging applications involved high peak power (> MW/pulse) transmitters such as Q-switched flashlamp pumped Nd:YAG systems to capture returns from retro-reflectors on LEO or MEO satellites. Multi-beaming is typically used to mitigate the scintillation effects of the atmosphere and also to allow lower power densities on the telescope optics with more readily available sources. For LEO based communication systems, moderate power (0.1 to 10 W) NIR fiber coupled diode lasers prove sufficient as beacon sources under cw or with low rate modulation.

The OPALS project involved four internally wavelength stabilized sources of 2.5 W each at 976 nm operated in cw mode to match the CCD based flight receiver requirements. Due to the broad beam widths, multi-spatial mode sources were sufficient.

The beacon lasers for the LLOT project required much higher powers for the lunar distances with narrower beam-widths. Hence, multiple fiber lasers with single mode output beams were utilized with low rate modulation to give an average laser output power of 60 W (10 W per beam) at 1568 nm, shown in Fig. 11. A master oscillator power amplifier architecture for each source was used but instead of the typical high rate modulated seed source, the final amplifier stage had direct modulation of the pump diodes synchronized at 1 kHz, enough for the flight system pointing and tracking quad sensor to lock onto for acquisition. Full monitor and control of the laser was possible remotely from the control room.

Future systems point to even higher powers required for use as an uplink or beacon source. A typical Mars optical communication system would require up to 5 kW of ground transmitted power around 1.03 μm.

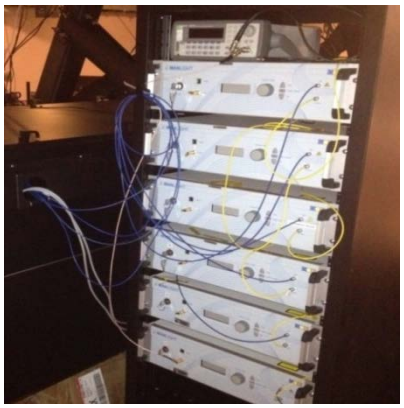

Figure 11 LLOT beacon laser system with six independent fiber based sources mounted in rack near optical bench.

VI. Laser Safety Considerations

Space to ground link demonstrations usually require the propagation of high power laser beams from the ground to act as beacon sources for the space laser communication terminals pointing narrow downlink beam-widths. The laser safety system at OCTL was developed to meet regulations for safe propagation of high power laser beams through navigable airspace and to protect space based assets from inadvertent illumination. Within the OCTL building, OSHA regulations for laser safety are followed but outdoor propagation requires the oversight of the FAA and USAF Laser Clearing House (LCH) under the US Strategic Command of the Joint Forces Space Operations Center (JFSpOC). The laser safety system incorporates a safety shutter that can be commanded to block the beam (see Figure 9 and 10), dumping the outgoing power to a beam block, either manually or autonomously from the beam monitoring system. The three tier system has been described in detail elsewhere[14] but underwent modifications for the recent demonstrations. Predictive avoidance (PA) files from the LCH were uploaded each day to a

LabVIEW based controller that shuttered the beam as needed throughout the pass for LLOT based on an extended avoidance cone around the narrow beacon beams. An example of the PA outages for a typical day is shown in Fig 12. There were up to four or five link opportunities for a given day, each of around 20 minutes at two hour intervals such that a PA event only rarely coincided with an active link.

For OPALS, on the other hand, the beacon beams are significantly wider with a FWHM of 1.6 mrad (compared to 40-100 μrad for LLOT) realizing much lower irradiance at the LEO orbiting ISS and avoiding the need for PA files.

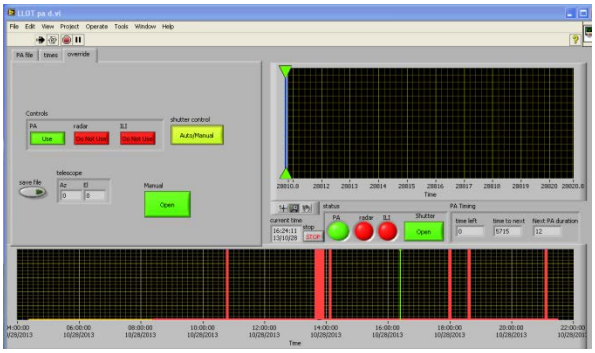

Fig 12 Laser safety control program showing PA outages (red) with shutter controller

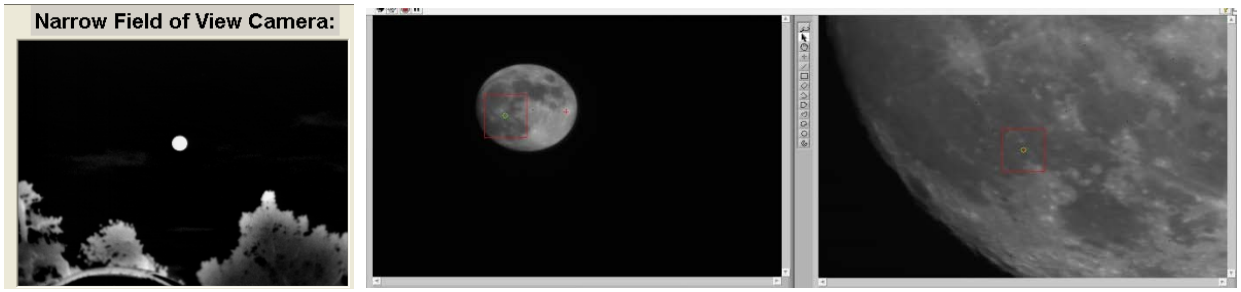

Fig 13 Moon imaged for laser safety system: a) LWIR camera, b) visible zoom camera, and c) visible camera on acquisition scope during an LLOT link opportunity.

The aircraft monitoring system radar was not operational for either experiment so a back-up system was in place that added outside observers along with a web based air traffic monitoring capability. The air traffic area around OCTL was monitored for incoming flights via commercial websites that captured most aircraft with on-board transponders. Other aircraft were noted by the external observer and monitored via the long wave infrared (LWIR) cameras, shown in Fig 13. Any traffic that entered the narrow field of view LWIR camera was also visible on a visible zoom camera co-boresighted with the main telescope and triggered the beam shutter. For LLOT, since a spacecraft in low-orbit around the moon was being tracked, aircraft over-flights entering the avoidance cone were readily discernible on the sky.

For OPALS this would prove problematic for direct viewing due to the fast slewing telescope. However, since the beams are IR and the NOHD is sufficiently close (60 m for full transmitted power); no beam shuttering will be necessary for aircraft avoidance.

In summary, the OCTL laser safety system can support safe transmission of high power lasers to meet all layers of government oversight.

VII. Conclusion

In this report operational considerations used at OCTL to support space-to-ground laser communications from near-Earth spacecraft have been described. The results achieved for LLOT and analysis used for OPALS have been reported elsewhere and are cited for readers who are interested in finding out more details. The description presented was the result of mission specific requirements that the ground station had to meet. However, as may be apparent to the reader there are underlying common functions and activities that future ground stations deployed for supporting laser communications operations from space will have to implement. As the technology matures

questions about multi-mission support and how to achieve this cost-effectively will become increasingly important. For example, can ground stations for supporting laser communications from space be coordinated and operated remotely from a centralized operations center. The experience gained from past, ongoing and upcoming demonstrations will provide answers to these questions. In the near future we hope to report on the experiences with the OPALS link demonstration.

Acknowledgments

The work described was carried out at the Jet Propulsion Laboratory (JPL), California Institute of Technology under contract with the National Aeronautics and Space Administration (NASA).

References

[1] Keith E. Wilson, Joseph Kovalik, Abhijit Biswas, Malcolm Wright, William T. Roberts, Yoshihisa Takayama, Shiro Yamakawa, "Preliminary results of the OCTL to OICETS optical link experiment (OTOOLE)," SPIE Proceedings on Free-Space Laser Communication Technologies XXII, [ed. Hamid Hemmati], 758703, 2010.

[2] J. Kovalik, A. Biswas, K. Wilson, M. Wright, W. T. Roberts, "Data Products for the OCTL to OICETS optical link experiments," SPIE Proceedings on Free-Space Laser Communication Technologies XXII, [ed. Hamid Hemmati], 75870C, 2010.

[3]"Laser Communications Relay Demonstration The Next Step in Optical Communications," NASA Factsheet, http://www.nasa.gov/pdf/742122main_LCRDFactSheet3.pdf.

[4] Don M. Boroson, Bryan S. Robinson, Daniel V. Murphy, Dennis A. Burianek, Farzana Khatri, Joseph M. Kovalik, Zoran Sodnik, Donald M. Cornwell, "Overview and results of the Lunar Laser Communications Demonstration," SPIE Proceedings on Free-Space Laser Communication Technologies XXVI, [ed. Hamid Hemmati, Don Boroson], 89710S, 2014.

[5] Daniel V. Murphy, Jan E. Kansky, Matthew E. Grein, Robert T. Schulein, Matthew M. Willis, Robert E. Lafon, "LLCD Operations using the Lunar Lasercom Ground Terminal," SPIE Proceedings on Free-Space Laser Communication Technologies XXVI, [ed. Hamid Hemmati, Don Boroson], 89710W, 2014.

[6] Abhijit Biswas, Joseph M. Kovalik, Malcolm W. Wright, William T. Roberts, Michael K. Cheng, Kevin J. Quirk, Meera Srinivasan, Matthew D. Shaw, Kevin M. Birnbaum, "LLCD Operations using the Optical Communications Telescope Laboratory (OCTL)," SPIE Proceedings on Free-Space Laser Communication Technologies XXVI, [ed. Hamid Hemmati, Don Boroson], 89710X, 2014.

[7] Zoran Sodnik, Hans Smit, Marc Sans, Igor Zayer, Marco Lanucara, Iciar Montilla, Angel Alonso, "LLCD Operations using the Lunar Lasercom OGS Terminal," SPIE Proceedings on Free-Space Laser Communication Technologies XXVI, [ed. Hamid Hemmati, Don Boroson], 89710W, 2014.

[8] Bogdan Oaida, William Wu, Baris I. Erkmen, Abhijit Biswas, Kenneth S. Andrews, Michael Kokorowski, Marcus Wilkerson, " Optical link design and validation testing of the Optical Payload for Lasercomm Science (OPALS)," SPIE Proceedings on Free-Space Laser Communication Technologies XXVI, [ed. Hamid Hemmati, Don Boroson], 89710U, 2014.

[9] Abhijit Biswas, Sabino Piazzolla, Bruce Moision, Douglas Lisman, "Evaluation of deep-space laser communications under different mission scenarios," SPIE Proceedings on Free-Space Laser Communication Technologies XXIV, [ed. Hamid Hemmati], 82460W, 2012.

[10] W. Thomas Robert and Malcolm W. Wright, "Deep-space Optical terminals (DOT) Ground Laser Transmitter (GLT) Trades and Conceptual Point Design," Inter-Planetary Network (IPN) Progress Report 42-183, November 15, 2010, http://tmo.jpl.nasa.gov/progress_report/42-183/183C.pdf

[11] Bogdan Oaida, William Wu, Baris I. Erkmen, Abhijit Biswas, Kenneth S. Andrews, Michael Kokorowski, Marcus Wilkerson, " Optical link design and validation testing of the Optical Payload for Lasercomm Science (OPALS)," SPIE Proceedings on Free-Space Laser Communication Technologies XXVI, [ed. Hamid Hemmati, Don Boroson], 89710U, 2014.

[12] Shaw, M. D., Stern, J. A., Birnbaum, K., Srinivasan, M., Cheng, M., Biswas, A., Marsili, F., Verma, V. B., Mirin, R. P., Nam, S.W., Farr, W. H., "Tungsten Silicide Superconducting Nanowire Arrays for the Lunar Laser OCTL Terminal," Paper: QM4L7, CLEO-2013 Technical Digest.

[13] Marsili, F. Verma, V. B., Stern, J. A., Harrington, S., Lita, A. E., Gerrits, T., Vayshenker, I., Baek, B., Shaw, M.D., Mirin, R. P., Nam, S. W., "Detecting Single Infrared Photons with 93% System Efficiency," Nature Photonics, 7, 201-214 (2013).

[14] K.E. Wilson, J. Kovalik, A. Biswas, and W.T. Roberts, "Development of laser beam transmission strategies for future ground-to-space optical communications," SPIE Proceedings on Atmospheric Propagation IV, 6551B, 2007.